Master thesis report

Stijn de Jong

Low cost disdrometer

Improved design and testing in an urban environment

December 2010

Committee:
Prof. Dr. Ir. Nick van de Giesen
Ir. Rolf Hut
Dr. Ir. Marie Claire ten Veldhuis

ClimateCityCampus
DRI environment

TU Delft
Delft University of Technology

Content

Preface

Early 2009 Coen Degen developed the first prototype of a low cost disdrometer. After his work I took over the further development and testing as a student assistant of the department, but I had also fun doing it. At the moment I had to look for a subject for my master thesis the possibility arose to take on the further development as a graduation project.

The main goal of the project was to go from one prototype to a number of, easy to build, low cost disdrometers. Especially the possibilities that occurs when you have a cheap rain gauge at your disposal arouse my interest. However the development of the sensor and logger for the disdrometer took more time as planned on forehand. This was mainly caused by problems in the development of the logger, the fabrication of the logger and the many software versions that had to be tested and debugged. At the time of writing this report there are still problems in the logger that are unsolved.

The measurements with the disdrometer which were done for this thesis unfortunately could not be used for the investigation of the spatial distribution of rain in an urban environment, but only could be used to define and solve some problems. Therefore the focus of this thesis had to change from develop and measure to only develop, making this project kind of unusual for a watermanagement student.

When you read this report you will find out that there is quite some work that has to be done before the low cost disdrometer operates as it should under all circumstances. Therefore I'm glad to mention that there are already students from different faculties working on projects where the low cost disdrometer is a part of.

The achieved work within this project would not be possible without the help of many. I hereby want to thank Kees van Beek for his help and commitment in developing the logger for the disdrometer, Rolf Hut and Nick van de Giesen for their guidance, and the department for the investments made.

Stijn de Jong

Summary

In 2009 the department of water management started with the development of a cheap rain gauge that is suitable for use in remote areas and tropical areas. The first prototype of this rain gauge was based on an acoustic disdrometer and an audio recorder was used for data acquisition. This disdrometer could be produced for only a fraction of the market price for a rain gauge with the same specifications. Because of the low price this disdrometer also lends itself for large scale application in urban area, where a lot of measurements are desired, because of the spatial distribution of rainfall.

The main objectives of this thesis are the improvement of the design of the sensor and data acquisition, testing the new prototype and develop a method to validate the measurements.

The design of the sensor has been improved in terms of sensitivity and the method of production. From the measurements it is observed that the smallest drop measured by the current prototype is 0.6 mm, where the smallest drop measured by the first prototype was 1.5mm. In the current prototype two negative effects are observed, the radius effect and the puddle effect, however these effects do not have a visible effect on the measurements.

Data acquisition with an audio recorder, which was used for the first prototype, requires a lot of data storage. This is mainly because the signal is measured continuously. Also the amount of energy needed is a disadvantage of the audio recorder. A new data logger was developed for the sensor to reduce the amount of data that has to be stored and to increase the time that the disdrometer is able to measure. The logger can be used in two configurations, as a standalone unit and in a setup with multiple disdrometers (Rainscan).

For the calbriation of the low cost disdrometer an expermental calibration setup is used. With this setup the outputs of the logger are linked to drops of known size. Calibration of the disdrometer showed a clear relation between the signal energy of a drop and the size of the drop. The uncertainty in the calibration curve can be decreased by calibrating the disdrometer with the help of an optical disdrometer.

The disdrometer gives an array of drop energies as output, from which a drop size distribution can be derived. A method is developed to validate the outcome of the low cost disdrometer, in terms of drop size distribution, if there are no other disdrometers available to compare to. With this method it is possible to get insight in the expected drop size distribution based on the data of a tipping bucket.

To test the low cost disdrometer in an urban environment two case studies were conducted. For each case study, one configuration of the low cost disdrometer was used. For the EWI case study the Rainscan configuration was used, where for the Singapore case study the standalone version of the disdrometer was used.

The results from the measurements in the case studies showed a large underestimation of the total amount of rain, which indicates an error in the design. Therefore the results are not used for any investigation of rainfall in the urban environment. Analyses show that this underestimation only takes place during rain events with high rain intensity. The maximum intensity measured with the disdrometer is 26mm/hr where the tipping bucket measured 150mm/hr. Several tests showed that this

underestimation is caused by an error in the logger of the disdrometer. So far it is unknown what the exact error is.

The main conclusion drawn from the conducted research is that the sensor of the current prototype performs better than the first prototype and that in general the principle works. However the logger designed for the disdrometer is not capable of giving a right representation of the reality under all circumstances. Before the low cost disdrometer can operate in the field for longer periods, first the problems with the data logger have to be solved.

Reader

Chapter 1: Introduction
Chapter 1 is an introduction and gives the necessary information about disdrometers in general, a description of two applications for which the low cost disdrometer is developed and a short description of the first low cost disdrometer prototype made by Coen Degen.

Chapter 2: Objectives
In this chapter the objectives of this master thesis are given.

Chapter 3: Design
Chapter 3 elaborates on the design of the low cost disdrometer. First the criteria are set and the negative and positive aspects of the first prototype are highlighted then the considerations made for the current prototype and the data logger are explained.

Chapter4: Calibration
Chapter 4 deals with how the disdrometer is calibrated. The calibration method is described, the calibration curve for the current prototype is given and an estimate for the uncertainty is determined. Also an alternative calibration method will be explained here.

Chapter 5: Validation
In chapter 5 a validation method for the didsdrometer is explained. With this method it is possible to get insight in the expected drop size distribution if there is no conventional disdrometer available.

Chapter 6: Case study
Chapter 6 describes the case studies that are performed with the low cost disdrometer.

Chapter 7: Results
In chapter 7 the results of the case studies are given.

Chapter 8: Analysis
The results of the case studies are analyzed in this chapter.

Chapter 9: Conclusion
The final conclusion.

Chapter 10: Future work
The development of the low cost disdrometer is an ongoing project. Future work that has to be done is described in this chapter.

1. Introduction

Early 2009, Coen Degen started with the development of a low cost raingauge. His assignment was to develop a raingauge that is simple, inexpensive and suitable for use in remote areas and tropical climates. The first working prototype made was based on the principle of an acoustic disdrometer. The request for such a device was born within the TAHMO-project, but the low cost disdrometer also lends itself for other large scale application, such as in urban area.

In this chapter some background information will be given about the principle of a disdrometer, the TAHMO project and the application of a low cost raingauge in urban area. Finally a short description of the first prototype will be given.

Disdrometer

In the glossary of the American Meteorological Society the term disdrometer is described as:

> *"An instrument that measures and records the sizes of raindrops. A common type of disdrometer consists of a sensitive transponder that measures the momentum of individual drops as they fall onto an exposed horizontal surface. Size is determined from momentum through calibration, and the drop-size distribution is obtained by keeping a tally of the number of drops in different size categories that fall onto the surface in a given period of time."*

In other words, a disdrometer is a raingauge that records the information of individual drops, this information adds up to a drop size spectrum, or a drop size distribution (DSD), over a certain period. From the drop size distribution over a certain period it is possible to calculate the total amount of rain and rain intensity. The drop size distribution itself is of interest for radar technology, since the drop size and the concentration of drops mainly determines the reflectivity of a cloud, from which the rain intensity can be determined. Also for research in erosivity by rainfall the DSD is of importance, since large drops cause more erosion than small drops. (Brandt 1990).

There are several types of disdrometers available on the market, the most common ones are the disdrometers that make use of optic or acoustic.

The acoustic disdrometer uses the same principle as an ordinary microphone and soundbox where respectively sound waves are converted in electric pulses or electric pulses are converted to sound waves. The vibration caused by a drop impact on an acoustic disdrometer is converted by a piëzo detector into an electric pulse which is the input for the microcontroller of the data logger.

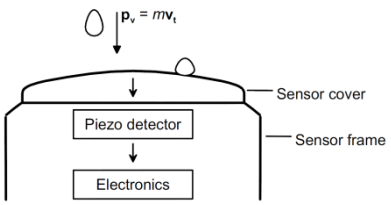

Figure 1: Principle of an acoustic disdrometer (Salmi and Ikonen 2005)

The optical disdrometer uses a beam of light to determine the size and speed of a raindrop. Light is transmitted at one side of the optical disdrometer and received at the opposite side by the receiver. If a raindrop passes the beam of light, the receiver will receive less light from the transmitter. The speed and size of a raindrop determines the time that the light beam is interrupted, and to which extend. Most optical disdrometers can, besides rain, also detect and distinguish other hydrometeors such as hail, graupel and snow.

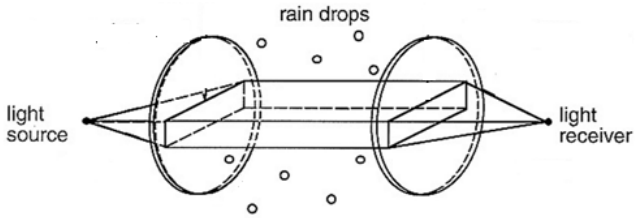

Figure 2: Principle of an optical disdrometer (Lavergnat and Golé 1998)

Low cost disdrometer

The price of a professional disdrometer on the market starts from €3000,-. For large applications these disdrometers are too expensive. The costs for the low cost disdrometer described in this report are just a fraction of the market price. The total cost of materials does not exceed €10, - and the cost of the logger is €70,-, but this cost will decrease if the disdrometer is produced in great numbers.

The low cost disdrometer is based on the acoustic disdrometer described by Joss and Waldvogel (Joss and Waldvogel 1967). The basis of the low cost disdrometer is a piëzo-electric element. The piëzo-electric element creates an electric pulse when it is deformed. The degree of deformation depends on the size of impact. In other words, the bigger the drop the larger the electric pulse. Figure 3 gives a schematic overview of how a drop impact is interpreted. At the moment of *drop impact* the piëzo-electric element deforms, creating a signal. The *drop signal* is defined as the signal given by the piëzo-electric element for one drop impact. The start of the drop signal is at the moment the signal exceeds the threshold for the first time. The end of the drop signal is defined as the moment the drop signal does not exceed the threshold for a certain period of time. The length of a drop signal depends on the drop impact and material properties. The length of the signal is approximately 5-15 ms.

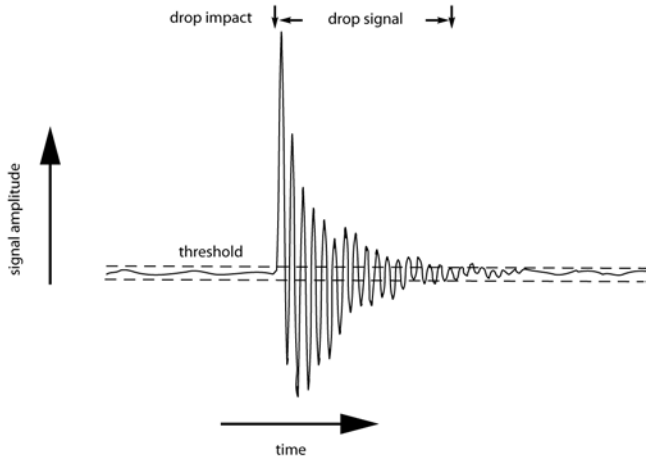

Figure 3: Schematic overview of drop interpretation

By calibration a relation between the drop signal and the drop diameter can be found. If the size of the individual rain drops is known, the total rain depth of a rainfall event can easily be calculated as follow:

$$R = \sum \frac{\frac{1}{6} * D^3}{{r_s}^2}$$

$$R = rain\ depth\ (mm)$$

$$D = equivalent\ drop\ diameter\ (mm)$$

$$r_s = radius\ of\ sensor\ (mm)$$

In the first prototype (Degen 2009) the piëzo-electric element is fixed between two parts of crystal clear cast resin (epoxy polymer) and finally encased by a PVC pipe to protect it from outside influences. Figure 4 shows a schematic overview of the first prototype. More details of the first prototype will be described in Chapter 3: Design.

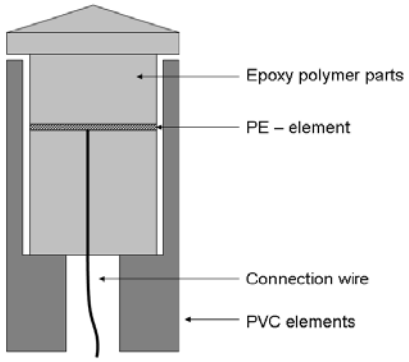

Figure 4: Schematic drawing of the first sensor prototype

The low costs make the disdrometer attractive to use for applications where funds are scarce and great numbers desired, such as the TAHMO project and the use in urban environments.

TAHMO

TAHMO stands for Trans-African Hydro-Meteorological Observatory and is an initiative by Nick van de Giesen (Delft University of Technology), John Selker (Oregon State University) and Marc Andreini (International Water Management Institute). “The goal of TAHMO is to better understand the African environment through participatory sensing, modeling and education”. One of the objectives is to create a network of 20.000 hydro-meteorological stations in Africa within the coming decade. The stations will be placed at schools and integrated in the educational program. The data obtained with this network will be combined with models and satellite observations to obtain a very complete insight in the distribution of water and energy stocks and fluxes within Africa.
Each hydro-meteorological station should measure climate parameters such as temperature, humidity, wind speed/direction, incoming and outgoing radiation and precipitation. Equipment to measure these parameters are available on the market but often very costly. To make this project possible each station should cost no more than $200,-. This has to be achieved by using innovative sensors and ICT. The low cost disdrometer is one of these sensors. (www.tahmo.org).

Urban

Automated hydro-meteorological stations are often placed at location where buildings are sparse, such as airfields. Figure 5 is a compilation of all automated hydro-meteorological stations of the Royal Dutch Meteorological Institute (KNMI). Even rainfall, the basic input for every hydraulic model, is often measured in an open field. Reason for this are the standards of the World Meteorological Organization (WMO) which state that a raingauge should be positioned at a distance at least two times the height of the nearest object (WMO 2008). However, information about precipitation in urban areas is desired to make better urban water management possible (Schilling 1991; Niemczynowicz 1999). There are clear indications that climate change and the urban heat island effect will cause more rain events with a higher intensity (Bornstein and Lin 2000), which make the need for information about precipitation in urban areas only becoming more important.
Disadvantage of rain measurements in urban areas is the spatial distribution of rain due to influence of buildings on wind and temperature. To obtain a statistically estimate of the total rainfall in an urban area the rain measurements with a high spatial resolution. The high initial cost of conventional rain gauges prevent that such measurements are carried out. The low cost disdrometer could be a solution to this problem.

Figure 5: Compilation of location hydro-meteorological stations KNMI (www.knmi.nl)

2. Objective

The main goal of this thesis is to develop a rain gauge which is affordable and robust, so it can be used for large scale applications, such as the Tahmo project and as a rain gauge in urban areas.

As mentioned in the introduction Degen started the development of such a raingauge by making a first prototype of an acoustic disdrometer. The work presented in this thesis is a continuation of his work and most objectives are based on the findings of his research. The objectives can be summarized in three words: **improve**, **test** and **validate**.

Improve
The sensor of the disdrometer have to be improved by implementing the findings of Degen into a new design of the sensor that can readily be reproduced.

The data acquisition of the disdrometer have to be improved. The audio recorder that is used for the first prototype have to be replaced by a data logger, to reduce the amount of data and to increase the time that the disdrometer is able to measure.

Improvement of the calibration of the sensor. Find a better way to calibrate the low cost disdrometer.

Test
The new design of the sensor and the data logger has to be tested. As a test two case studies are performed in an urban environment.

Validate
Develop a validation method to check the measured drop size distribution. A disdrometer provides information about the size of the individual drops. A validation method has to be developed to check this information on plausibility if there is only information of volumetric rain gauges available, and no direct independent measurement of drop size distribution.

3. Design

In this chapter the design of the low cost disdrometer will be described and discussed. After the criteria of the design are given, the advantages and disadvantages of the first prototype are discussed. Finally I will elaborate on the considerations made for the current prototype and the accompanying data logger. Also the short comings of the current design and possible alternatives are discussed.

The design has been an iterative process and only the first and current prototype will be described in detail in this chapter. Pictures and short descriptions of the prototypes which were made during the development process are given in Appendix 1: Prototypes.

A step-by-step description of the production and installation of the low cost disdrometer and the data logger are given in a separate manual.

3.1 Criteria

The raingauge will be used on large scale in remote areas with tropical climates (Africa), but also in urbanized areas. It is therefore important that the raingauge is relatively cheap and does not need much maintenance.

Based on these constraints the following criteria are formed:

- The sensor should not contain moving parts or parts that clog.
- Most of the material used should be readily available, to prevent high costs due to custom made parts.
- Data acquisition has to be efficient. Large amounts of data per rain event would increase the cost of data storage and it would be difficult and/or expensive to read the data from a distance.
- The sensor should be easy to (re)produce.
- The sensor has to be durable.

3.2 First prototype

A schematic overview of the first prototype of the low cost disdrometer is given Figure 6 (Degen 2009).

The basis of the sensor is a piëzo electric (PE) disk that produces a voltage signal upon deformation by an impacting rain drop. The PE element is fixed between two parts made of epoxy polymer and finally encased by a PVC pipe to protect it from outside influences.

The voltage signal of the sensor is transmitted to an audio recorder through a co-axial wire. The raw data were stored in a wave file with a sample frequency of 16 kHz. Disadvantage of an audio recorder that it records continuously, also if there is no rain. The amount of data, in terms of size, is enormous compared to the amount of information which it contains. For one hour of data approximately 0.75GB is needed for storage. The raw data was post processed with MatLab, for which an empirically derived calibration curve was used. The smallest drop diameter used for calibration was 2mm.

Six sensors of this prototype were produced manually using silicon rubber moulds. Due to this production process the sensors were not equivalent, causing measurable differences in impact responses between the sensors.

After a certain period, the PE element started “rusting”, this seems to be a negative effect of the use of epoxy polymer as a fixation material. The exact effect of the corrosion on the electric signal is unknown, but in terms of durability this effect is not desired.

Tests carried out with the first prototype showed that the sensor performs better than a tipping bucket for high rain rates, but that there is an underestimation of 20% for accumulated rainfall at low rain rates. This underestimation is mainly due to loss of signal for very small drops (Degen 2009).

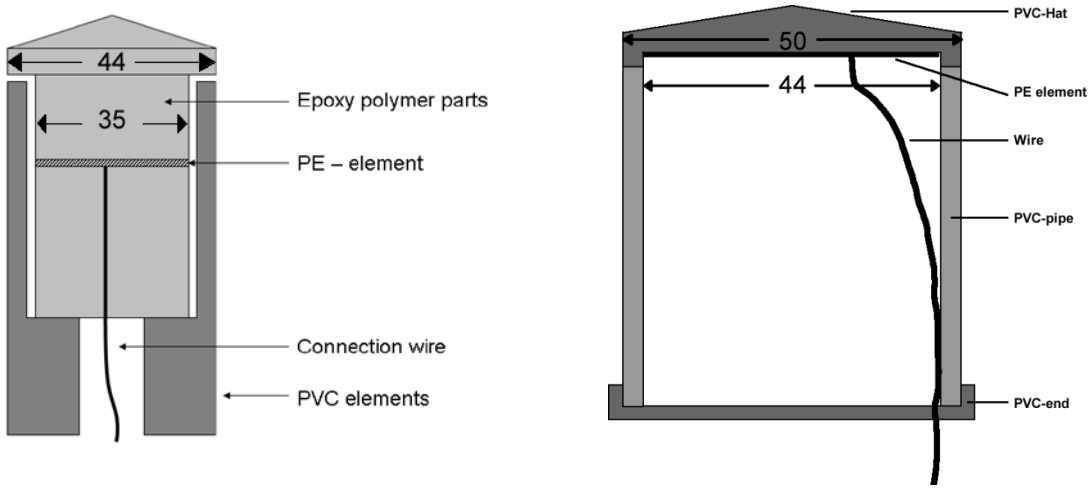

Figure 6: Schematic overview of first prototype (left) and current prototype (right)

3.3 Current prototype

Figure 6 gives a schematic overview of the current prototype. For each part of the sensor is explained which considerations were made, which shortcomings were observed, and possible alternatives are given.

The data acquisition of the current prototype is done by a newly developed logger. The logger processes the signal of the sensor and only stores the necessary data. A short explanation of the considerations made by the design of the logger and the development of the software are described below.

3.3.1 Sensor

The sensor exists of three main parts; the piëzo-electric disk, the pvc casing and the hat of the sensor.

Piëzo-electric disk

The design parameter of the piëzo-electric disk is the desired surface area of the sensor. The surface area of the sensor is a compromise between two opposite specifications. For a larger surface area the ratio of drops hitting the edge and not giving a full impact is less than for a smaller surface area. On the other side for a bigger surface area the chance of simultaneous drop impacts increase, causing a wrong interpretation of the signal.
A compromise between these two specifications is a sensor surface area of 90mm (Salmi and Ikonen 2005). The piëzo electric disk chosen for this prototype is 44 mm and is the biggest piëzo electric disk

that is readily available. Larger piëzo electric disks have to be custom made and this would increase the cost.

PVC
PVC is chosen as the basic material around the piëzo-electric disk. The advantage of PVC is that it is easy to make a water tight junction between two pieces with PVC glue. The use of silicone is not recommended since the acidity has a corrosive effect on the piëzo-electric disk, this effect is not observed for PVC glue.

The PVC pipe is the part where the sensor can be attached to a standard. The length of the pipe is chosen on the basis of practical considerations.

Hat
The hat of the sensor is the only part that is not readily available. For the hat it is important that the dimensions are about the same size as the piëzo electric disk and that the piëzo electric disk can be mounted on a flat surface.

In first instance, the hat was made of crystal-clear cast resin formed in a silicon mold. The piëzo electric disk was mounted with the same crystal-clear cast resin. Problem of this method is that the production of one hat is time consuming. The manual labor involved in producing such a hat makes it difficult to make two exactly the same products.
The hats of the current prototype are produced mechanically to reduce the variety between them.

An aluminum and PVC hat were tested in the lab. Based on the lab tests it was decided to use the PVC hat, because the observed output signal was twice as high as in case of the aluminum hat. PVC is also a cheaper material then aluminum.

Short comings
Two important short comings in the design, which were observed during the calibration process, but have to be mentioned here since it concerns the design of the hat as well, is the choice for the piëzo-electric element. The short comings can be described as the *radius effect* and the *puddle effect.*

Radius effect
A small test with bearing-balls indicated that the place of impact is very important for the type of signal and amount of signal energy. This test was conducted with bearing balls, because they are easier to handle and to aim at a specific distance from the center. This test also cuts out the variance between different drops, so the sensor is the only thing that is contributing to this effect.
The hat is divided in 10 intervals of 0.5cm, where 1 and 10 are the outer intervals. From the signals it is clear that the place of impact does have an important effect on the amount of signal, See Figure 7. It is clear that the amount of signal energy is strongly reduced when the place of impact is further away from the center of the sensor. This effect is also observed by (Licznar, Łomotowski et al. 2008). This effect should be kept in mind during calibration and data interpretation.

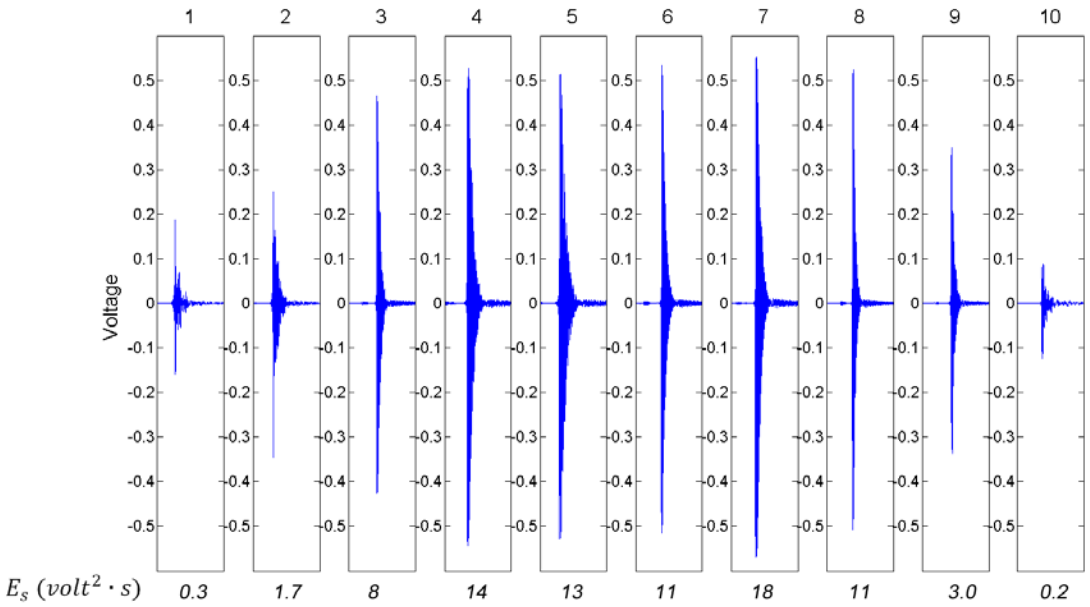

Figure 7: Radius effect, signal energy $(volt^2 \cdot s)$ given per place of impact

Puddle effect

During the calibration process and field tests it is observed that water remains on top of the hat of the sensor. This definitely influences the impact of a drop on the surface. This effect is mainly observed during drizzle, it is unknown how this effect develops during more severe rain events.

To reduce the effect of water adhering to the hat, the hat could be made of Teflon.

Figure 8: Little puddles on top of the sensor

3.3.2 Logger

Data acquisition with an audio recorder, which was used for the first prototype, requires a lot of data storage. This is mainly because the signal is measured continuously, so also when there is no rain data are still collected. Also the amount of energy needed is a disadvantage of the audio recorder, on average the batteries of the audio recorder have to be replaced every 8 hours.

A new data logger was developed for the sensor to reduce the amount of data that has to be stored and to increase the time that the disdrometer (sensor+logger) is able to measure.

Information about the electronic scheme of the logger and how to connect the logger to the sensor can be found in the manual. The most important information about the hardware and the software of the logger is described here.

NOTE: From the tests carried out with the disdrometer it appears that the logger is not capable to work correctly for high rain intensities. See chapter 8: Analysis.

Hardware

It is possible to connect one sensor to each logger. The logger can be used in two configurations; as a standalone and in Rainscan mode. In a standalone configuration the logger can be used without an external data storage and power supply. In the Rainscan configuration, multiple disdrometers can be connected to one data storage, which is not possible for standalone configuration.

The logger for the disdrometer is designed in such a way that the basis is the same for the standalone version and the Rainscan version. If the logger is used in the Rainscan method, only the basic design can be used. For using the logger as a standalone, the logger has to be extended with a SD-deck and a clock.

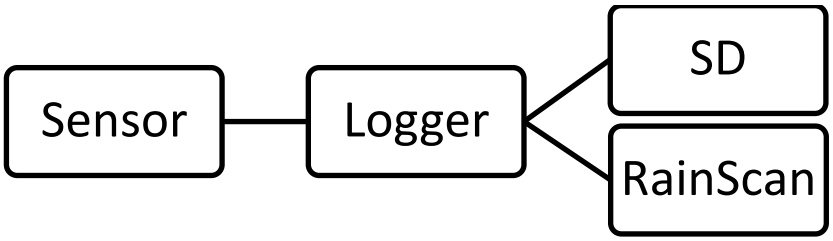

Figure 9: Schematic representation of data acquisition

RainScan

In the Rainscan configuration the disdrometers are connected in parallel. An additional module is necessary that communicates with the loggers and transfers all data to one central computer.
The logger of each disdrometer stores the recorded drop energy in an internal memory. The RainScan module addresses the first disdrometer, downloads the available data, sends the data to the computer and then does the same with disdrometer two, three, etc.

Each package of data that is downloaded from a logger receives a timestamp from a computer. In this way it is not necessary for each logger to have an own internal clock and the amount of data that has to be transferred from logger to computer is much less. A program on the computer stores the collected data for each disdrometer in a separate file.

Sample frequency
The sample frequency of the logger is 50kHz. The dominant frequency of a drop signal is around 2.5 kHz. According to the Nyquist principle a sample frequency of twice the signal frequency is needed to reproduce the signal. However to prevent the loss of information more samples per peak are necessary. Therefore it is chosen to oversample the dominant frequency with a factor 20.

AD-converter
After amplification the signal is in the range of -2.5-2.5V. The logger uses a 16 bits AD converter, so each sample value range from -32768 to 32768.

Filter
Before the signal enters the AD-converter, a bandpass filter is applied to filter out low and high frequencies which can cause a wrong interpretation of the signal. The cut off frequency of the high pass filter is 308 Hz, the cut off frequency of the low pass filter is set 19 kHz.

Software
The most important function of the software is the interpretation of the signal by the logger. In this stage of development it was important to retrieve as much information as possible. Therefore it was decided to not only look at the peak voltage of each signal, as described by (Henson, Austin et al. 2004), but to look at the complete signal. The algorithm used in the software of the logger determines the total energy of each drop signal.

The *drop signal* is defined as the signal given by the piëzo-electric element for one drop impact. The start of the drop signal is the moment the signal exceeds the threshold for the first time. The end of the drop signal is defined as the moment the drop signal does not exceed the threshold for a certain period of time, in this case 3 ms. The length of a drop signal depends on the drop impact and lies between approximately 5-15 ms.

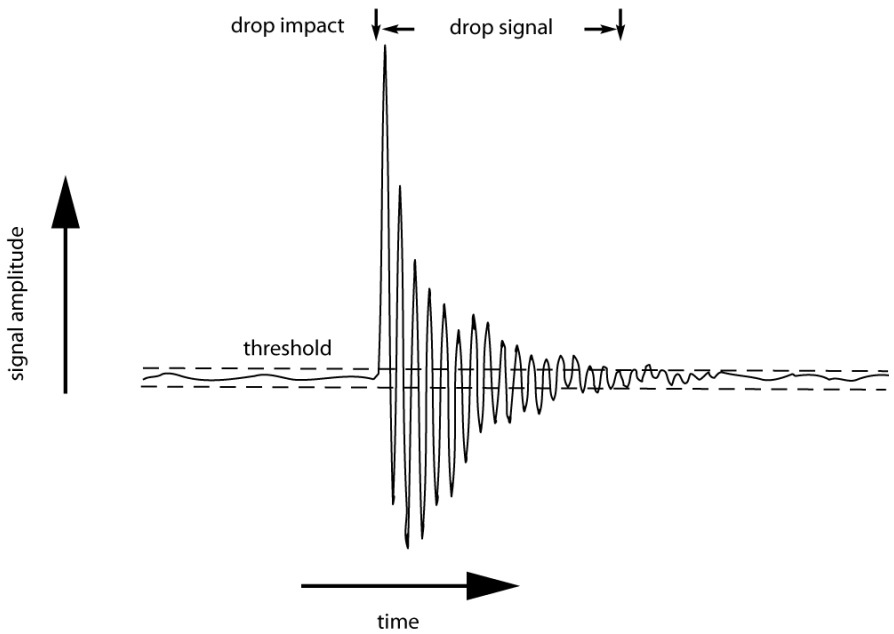

Figure 10: Interpretation of a signal by the logger

The total energy of a signal E_s over the time interval $t_1 \leq t \leq t_2$ in a continuous-time signal $x(t)$ is defined as (Oppenheim and Willsky 1997):

$$E_s = \int_{t_2}^{t_1} |x(t)|^2 \, dt$$

The logger takes samples of the signal, so the signal is not continuous, but a discrete signal. The total energy E_s over the time interval $n_1 \leq n \leq n_2$ in a discrete-time signal $x[n]$ is defined as:

$$E_s = \sum_{n=n_1}^{n_2} |x[n]|^2 \cdot \Delta t$$

$$\Delta t = \frac{1}{fs} = sample\ time$$

$$fs = sample\ frequency\ (Hz)$$

Determining the total energy with this algorithm consumes a relatively large amount of calculation space and is therefore not the most energy efficient one. Because the used logger should be capable of handling the needed amount of calculation capacity it is chosen to use this algorithm, since it reflects the total signal energy the best.

The output given by the logger is reduced by 2 bytes (divided by 256), to make sure that the sum of the squares does not exceed the 64 bits available for the storage of values.

Alternative

To reduce the time and space needed for a calculation, two algorithms could be used. The so called peak detection, where only the peak values are squared and summed, and the sum of all values. With both algorithms there is a clear relation with the full integral of the signal. See Figure 11 and Figure 12.

Peak detection: $E_{peak} = \sum_{n=n_1}^{n_2} |p|^2$, for time interval $n_1 \leq n \leq n_2$, where p is the maximum value of each peak in the signal

Sum of values: $E_{sum} = \sum_{n=n_1}^{n_2} |x[n]|$, for time interval $n_1 \leq n \leq n_2$

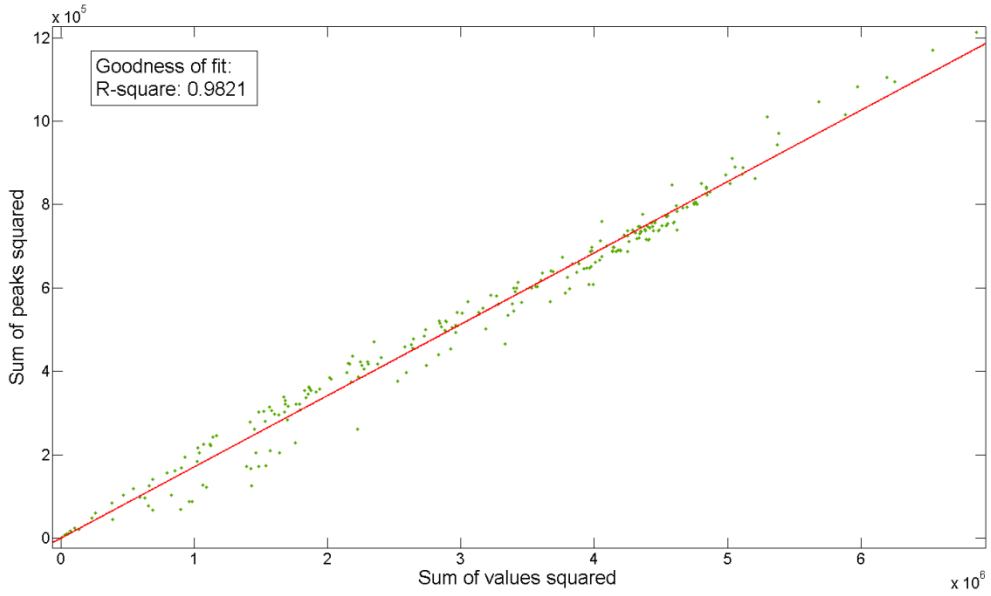

Figure 11: Relation between two algorithms to determine the energy of the drop signal; Sum of values squared (full integral of squared signal) vs. sum of peaks squared (peak detection)

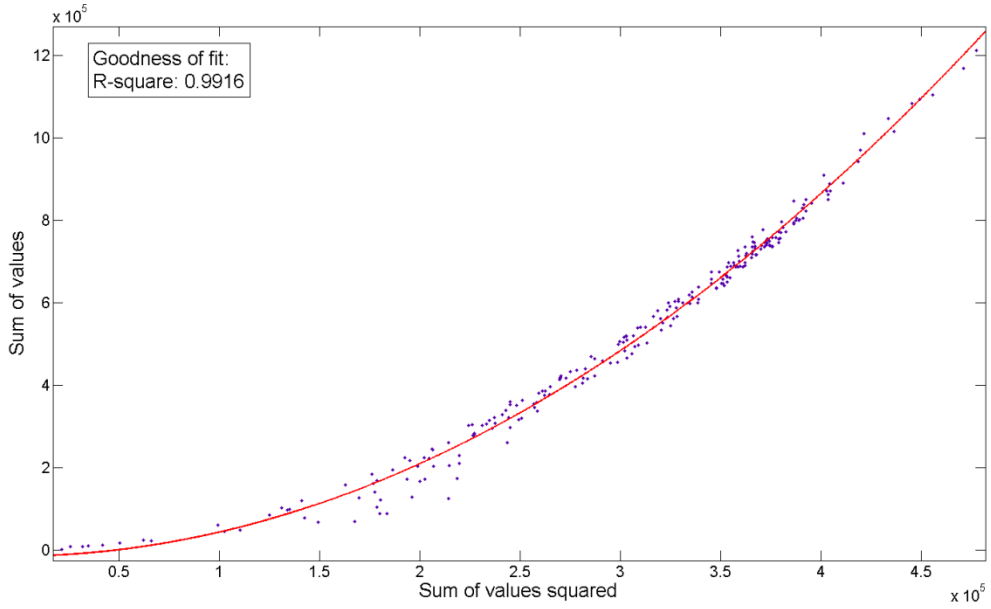

Figure 12: : Relation between two algorithms to determine the energy of the drop signal; Sum of values squared (full integral of squared signal) vs. sum of values (full integral of absolute signal)

4. Calibration

Calibration of the low cost disdrometer is needed to obtain a relation between the observed signal energy of a drop impact and the size of the drop. There are several ways to calibrate a disdrometer for example in the lab with a drop tower or outside with the use of other rain gauges. (Kourtellis, Kasparis et al. 2005) describe a way to calibrate their disdrometer with the information of a totaling rain gauge. With this method only the total volume of the reference rain gauge would be linked to the information of the disdrometer, but no direct insight in the signal-drop relation would be obtained. Therefore the calibration of the disdrometer was conducted in a laboratory with a drop tower. This chapter describes the experimental setup of the calibration and the calibration curve which is used for further measurements.

NOTE: The calibration was excecuted with the datalogger.In a later stage it was concluded that the logger does not performs as it should during rain events. In the lab these problems with the logger were not observed, therefore the derived calibration curve will be used for further analysis.

4.1 Method

For the calbriation of the low cost disdrometer described here, an expermental calibration setup is used. With this setup the outputs of the logger is linked to drops of known size.

Figure 13: Stairway Faculty of Civil engineering

Important constraint for the calibration is that the drops that hit the sensor have to reach terminal velocity before impact. The amount of energy of a signal depends on the mass and velocity of the drop. The terminal velocity of a drop is the velocity of the drop when the forces downwards are equal to the forces, due to resistance, upwards. It is assumed that rain drops reach this velocity, before they hit the surface. The terminal velocity depends on the size of the drop. Before the larger drops reach terminal velocity it has to be in freefall for at least 12 meters (Beard 1976).

The calibration of the disdrometer was conducted in a stairway of the Faculty of Civil engineering, Delft University of Technology. The stairway is located on the East side of the building and has a height of approximately 14 meters.

A reservoir is placed at a height of 12 meters from the ground. For the creation of drops medical needles in the range of 0.3-1.1mm are used. The needle is connected with a hose to the bottom of the reservoir. It is assumed that the drops from the needle are constant when the needle is fixed in rotation, angle and distance with respect to the water level in the reservoir. The size of the drops has to be determined for each batch of drops. When a batch is smaller than 1000 drops the decline of the water level during a batch can be neglected. For drops of 5mm in diameter 2000 drops are needed to let the water level drop 1mm.

The drop size is determined by catching an amount (100+) of drops with a small measuring cup, assuming that the size of a drop is constant, the volume of one drop can be determined by dividing the total volume by the number of drops. Due to the forces on a falling drop, a drop does not have the shape of a perfect sphere, and certainly not the typical paisley shape. For larger sized drops the shape looks more like a hamburger, see Figure 14 (Mason 1978; Beard and Chuang 1987), therefore the drop size is expressed as an equivalent diameter. The equivalent diameter, is the diameter of the drop if it would have been a perfect sphere.

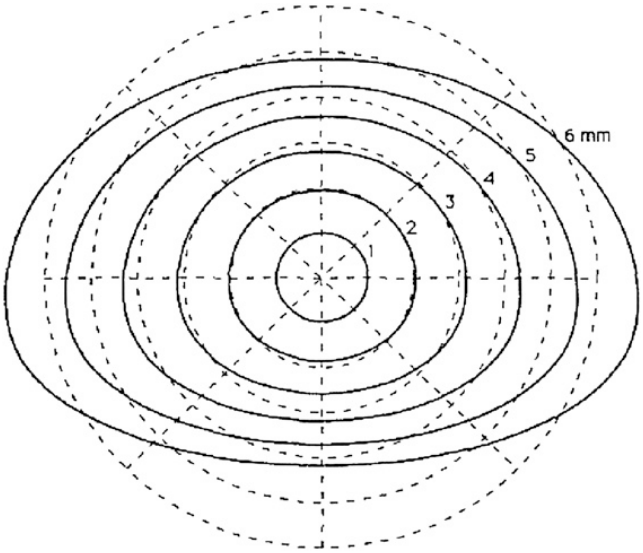

Figure 14: Shape of drops for certain sizes (Beard and Chuang 1987)

4.2 Calibration curve

The piëzo electric effect is understood as a linear electromechanical interaction between the mechanical and electrical state (Gautschi 2002). (Uijlenhoet and Stricker 1999) state that the hydrologically relevant properties of individual raindrops, namely terminal fall velocity, volume, mass, momentum and kinetic energy, can each be written as a power of the raindrop diameter. It is therefore evident that the calibration curve is also a power law.

$$f(D) = a * D^b$$

$$D = equivalent\ drop\ diameter\ (mm)$$

$$f = output\ of\ disdrometer$$

Knowing the drop size, and assuming terminal velocity, the impact of the drop is measured and logged with a disdrometer at the bottom of the stairway. This is done for different drop sizes in the range of 2-6mm. The coefficients for the expected power law are derived with the least square method:

$$f(D) = a * D^b$$

$$a = 1523.6$$

$$b = 6.598$$

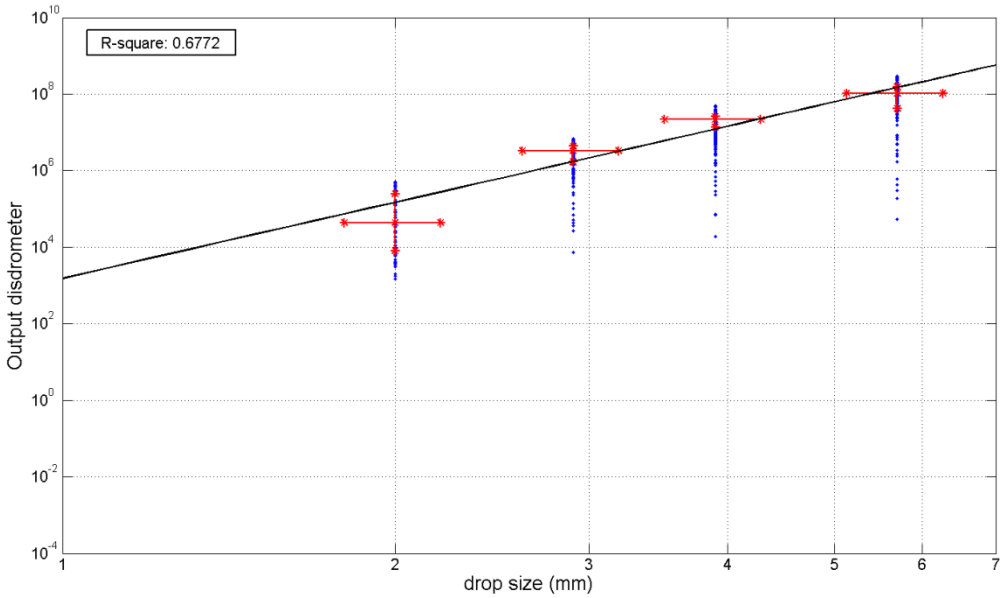

Figure 15: Calibration curve; blue: data points, black: fit through data points, red: first quartile (vertical), 10% margin drop diameter (horizontal)

The calibration method described above is performed for a number of disdrometers, for each disdrometer the output for a specific drop was in the same order of magnitude. Because the variance in output, for a specific drop diameter, seems larger than the variance between disdrometers it is assumed, for now, that the observed calibration curve is applicable for every disdrometer of this type.

4.3 Uncertainty

The uncertainty in the calibration curve is caused by several sources of error.

The largest source of error is how the drop size is determined. Drops are collected in a measuring cup. The number of drops collected is determined by counting the drops. The chance of miscounting the drops is, given the speed of the drops leaving the needle, significant. The measuring cup itself has a 0.1ml ruler, a misread of 0.1ml can already cause a 5% difference in drop diameter. The relative error for determination of the drop size is assumed to be +-10%.

In the calibration it is assumed that all drops of one batch have the same diameter if the needle stays in the same position. The stairway where the calibration is conducted is not a controlled environment, cracks and door openings cause some air turbulences in the stairway. This turbulence could influence the moment a drop is released from the needle. Due to this effect the sizes of the drops within a batch

will differ. This turbulence also could have an effect on the terminal velocity of the drops. The error caused by this effect is difficult to quantify, but it is probably one of the reasons why there is a large spread in the output for one drop size, see Figure 15.

The radius effect and puddle effect, described in chapter 3: Design, will probably have the largest contribution in the spread of output for one drop size.

During field tests it appeared that the logger did not work correctly in all cases. However given the low drop rate (+- 1 drop/second) during calibration, the logger did not have a problem interpreting all drop signals in the correct way. Therefore, the logger did not cause errors during the calibration.

The calibration curve is based on measurements with drop sizes in the range of 2-6mm, because it was not possible to create smaller drops. Therefore the curve had to be extrapolated. The error introduced with this extrapolation is hard to quantify, but considered smaller than the 10% associated with drop size determination.

Although there are quite some sources of errors in the calibration. The output-drop size relation seems to give good results, see chapter 8: Analysis.

4.4 Alternative method

An alternative calibration method is making use of photography. With this method it is possible to determine the size and velocity before impact and the place of impact. This could give more insight in the obtained calibration data.

For this setup, see Figure 16, a Stopshot module was used (http://www.cognisys-inc.com). The Stopshot module is able to trigger two flashes with a certain delay after it is activated by an infrared sensor. The infrared sensor activates the Stopshot module when the infrared beam is interrupted by a passing drop.

The camera used in this set up is a Canon Powershot, which was hacked with help of software found at: http://chdk.wikia.com. The hacked camera made it possible to make a sequence of photos and to adjust the shutter time to any desired length.

The camera is positioned in a dark box and the shutter time is set to 15 sec. The Stopshot module triggers two flashes quickly after each other, when the infrared sensor is triggered. In this way the drop will be on the photo twice. From the distance between the 'two' drops it is possible to calculate the velocity. Results of this setup are shown in Figure 17.

Although tests with this method were performed, they were not used for the final calibration. In the test environment, tests with small drops were not successful. Small drops drift easily by the turbulence in the stairway, which make triggering the sensor a very time intensive activity.

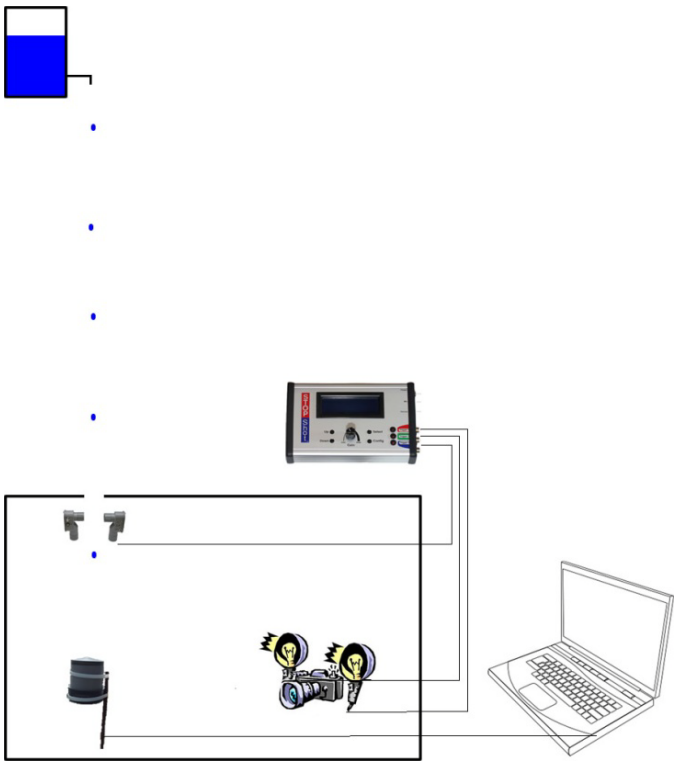

Figure 16: Schematization of photo calibration set up

Figure 17: Example of result photo calibration

5. Validation

The drop size distribution (DSD) is a frequency distribution of rain drop sizes. The DSD gives information on the frequency in which a specific drop size occurs, in other words if there are relatively more small or larger drops in a given rain event or cloud. The DSD is characteristic for the intensity of a rain event and is used in radar technology to link the reflectivity measured by the radar to the rain intensity.
The disdrometer gives an array of drop energies as output, from which a DSD can be derived. The easiest way to validate the DSD of the disdrometer is to compare it with the measurements of another, already established, disdrometer. This chapter describes a method to validate the outcome of the low cost disdrometer, in terms of DSD, if there are no other disdrometers available to compare to. With this method it is possible to get insight in the expected drop size distribution based on the data of a tipping bucket.

Method

Already in 1948 Marshall and Palmer published a short paper about the distribution of raindrops with size. Based on experimental observations they formulated a general exponential relation for the number of drops per cubic meter of air,N_V. The value for N_V, for $D = 0$, is equal to N_0. The number of drops per cubic meter depends on the rain rate, the rain rate is dealt with in the parameter Λ. (Marshall and Palmer 1948). This formula is still used as the basis to relate radar reflectivity to a certain rain rate.

$$N_V(D) = N_0 \exp(-\Lambda D)$$

The exponential relation stated by Marshall and Palmer is physically not applicable for small drops, since the number of drops for $D = 0$ is not equal to zero.

Uijlenhoet and Stricker combined the definition of the DSD, the number of raindrops with a certain diameter present per unit volume of air.(Marshall and Palmer 1948), and the power law relationship for the terminal fall speed in still air and raindrop diameter, to derive the raindrop size distribution at the ground. (Uijlenhoet and Stricker 1999)

$$v(D) = \alpha D^{\beta}$$

$$N_A(D) = \alpha N_0 D^{\beta} \exp(-\Lambda D)$$

$\beta = 0.67$ and $\alpha = 3.778\, ms^{-1} mm^{-\beta}$ are empirically derived using the data of Gunn and Kinzer. These values for $v(D) = \alpha D^{\beta}$ provide a close fit in the range of $0.5 \leq D \leq 5.0\, mm$ (Gunn and Kinzer 1949).

Since β is fixed, the only variable in the probability density function is Λ (mm^{-1}) which depends on the rain rate $R(mm\, hr^{-1})$ (Uijlenhoet and Stricker 1999).

$$\Lambda = 4.23 R^{-0.214}$$

$N_A(D)$ is the distribution of the total raindrop arrival rate over all raindrop sizes. Integration of $N_A(D)$ with respect to D gives an expression for the raindrop arrival rate $\rho_A(m^{-2}s^{-1})$. The raindrop arrival rate indicates how many drops arrive at the surface per unit of time.

$$\rho_A = \int_0^\infty N_A(D)\mathrm{d}D = \alpha N_0 \frac{\Gamma(1+\beta)}{\Lambda^{1+\beta}}$$
$$where, \Gamma\ denotes\ the\ gamma\ function$$

$N_A(D)$ can be interpreted as the product of the expected raindrop arrival rate $\rho_A(m^{-2}s^{-1})$ and the probability density function of the diameter $f_{D_A}(D)$.

$$\begin{cases} N_A(D) = \rho_A f_{D_A}(D) \\ f_{D_A}(D) = {\rho_A}^{-1} N_A(D) \end{cases}$$

The probability density function becomes:

$$f_{D_A}(D) = \frac{\Lambda^{1+\beta}}{\Gamma(1+\beta)} D^\beta \exp(-\Lambda D)$$

$$\beta, \Lambda > 0; D \geq 0;$$

This probability density function is a gamma distribution with $\frac{1}{\Lambda}$ as the scale parameter and $(1+\beta)$ as the shape parameter.

Figure 18 shows the probability distribution function for three different rain rates. From this figure it is clear that during a rain event with a high rain rate, there are relatively more larger drops as in a rain event with a low rain rate.

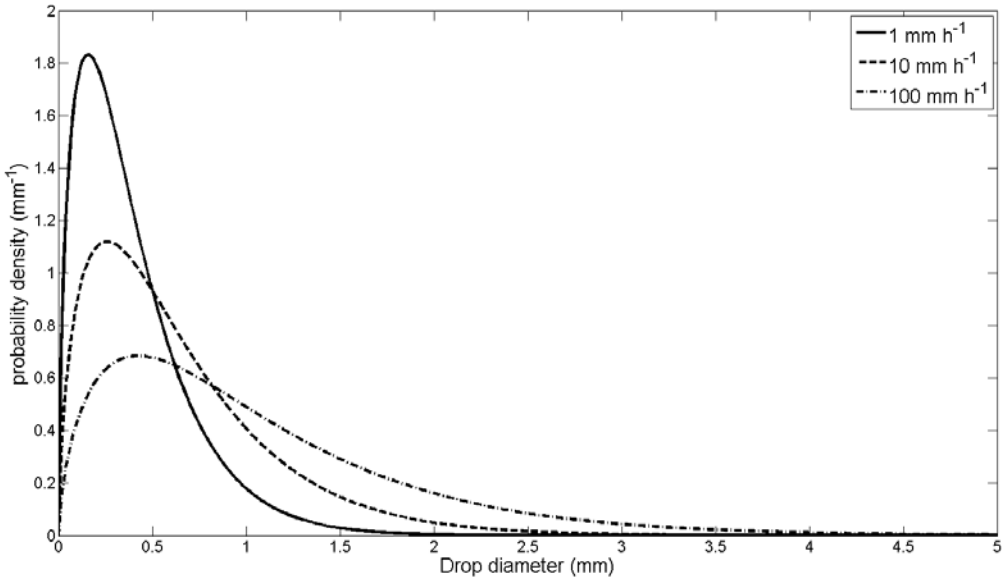

Figure 18: Probability density function of equivalent spherical diameter D of raindrops arriving at a surface per unit area and per unit time for different rain rates (Uijlenhoet and Stricker 1999)

The theory described above can be used to simulate a drop size distribution of a rain event if only the rain rate is known.

A rain event does not have one constant rain intensity. A rain event is build up from small parts with different rain intensities. To calculate the rain intensity for all those parts, the assumption made here is that each tip of the tipping bucket represents a constant rain depth (mm). From the time between two tips the different rain intensities in one rain event are determined.

$$R[\mathrm{n}] = \frac{h_{tip}(mm)}{t_{tip[n+1]} - t_{tip[n]}}$$

$$R = rain\ intensity\ (mm \cdot hr^{-1})$$
$$h_{tip} = rain\ depth\ of\ one\ tip\ (mm)$$
$$t_{tip} = time\ of\ the\ tip\ (hr)$$
$$n = number\ of\ the\ tip$$

For each determined rain rate a probability density function can be formulated. From this probability density function a number of 'drops' is selected randomly. The total number of drops selected has to add up, in terms of volume, to the volume of one tip. In fact a drop size distribution for the specific tip is determined. If this is done for all rain rates, a drop size distribution for the total rain event can be produced from all selected drops.

Uncertainty

The uncertainty of this method depends on the uncertainty of the tipping bucket data. The manufacturer of the tipping bucket specified 1% accuracy for rain rates up to 20mm/hr. For higher rain rates, the tipping bucket is less accurate because it tends to miss rain due to splashes.

Because of the uncertainty in the data of the tipping bucket this validation method is only used as a method to see if the data of the disdrometer is plausible.

Example

With a short example, the method described above will be explained. In this example the data obtained by Coen Degen in July 2009 are used. During this rain event of approximately 90 minutes a total rain depth of 23 mm was reached. During this rain event there was a peak intensity of 110 mm/hr. The lowest intensity observed was 1 mm/hr. Figure 19 shows how the rain intensity changed during the rain event.

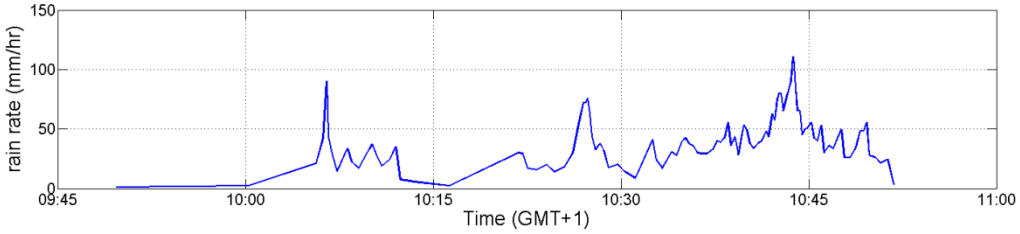

Figure 19: Rain rate during rain event 07/07/2009

Rain intensity is derived from the data obtained by a tipping bucket. The rain dept per tip is 0.2mm. From the time between two adjacent tips, and the rain depth per tip, the rain intensity for each tip can be calculated.

If the rain intensity is known the parameters for the corresponding probability function can be computed. For a rain intensity of 110 mm/hr:

$$\Lambda = 4.23 * 110^{-0.214} = 1.547\ (mm^{-1})$$
$$\beta = 0.67$$

$$f_{D_A}(D) = \frac{1.547^{1.67}}{\Gamma(1.67)} D^{0.67} \mathrm{e}^{(-1.547D)}$$

The probability density functions for each tip are shown in Figure 20. The probability density function corresponding to the highest intensity (110 mm/hr) of this rain event is highlighted by the red line in the figure. The probability density function corresponding to the lowest intensity (1 mm/hr) of this rain event is highlighted by the black line.

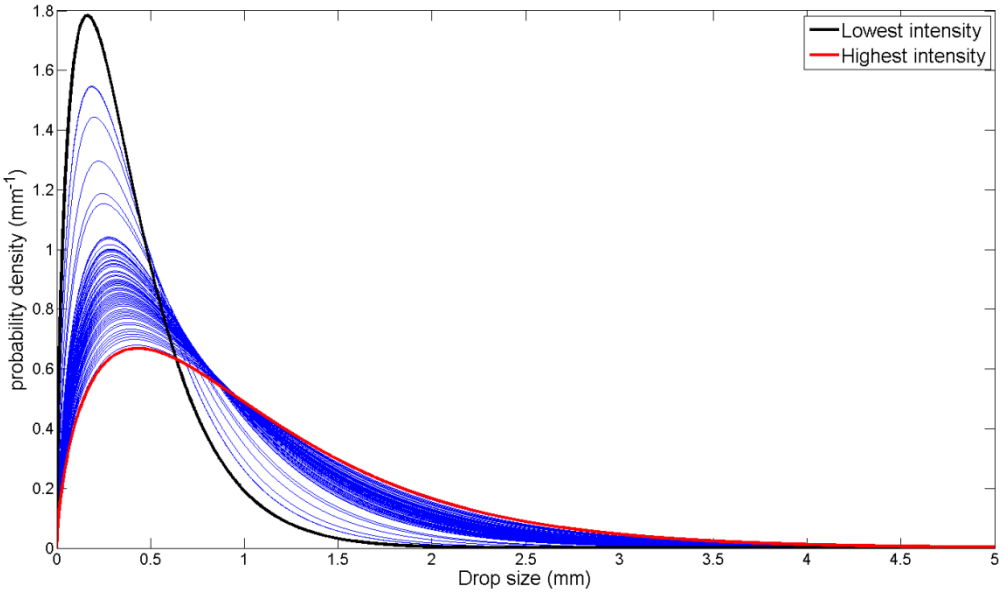

Figure 20: Probability density curves for individual rain intensities during rain event of 07/07/2009

From these probability density functions drops with a certain drop size are selected randomly. For each probability density function, the drops are selected until the total rain depth of the selected drops on the surface area of the sensor is equal to the rain depth of one tip, in this case 0.2mm.

The total of drops selected from all the probability functions is the drop size distribution of the rain event. Figure 21 shows the drop size distribution obtain with the method described above, indicated by the red line. The drops measured by Degen for this rain event are shown in the same figure, indicated by the blue bars.

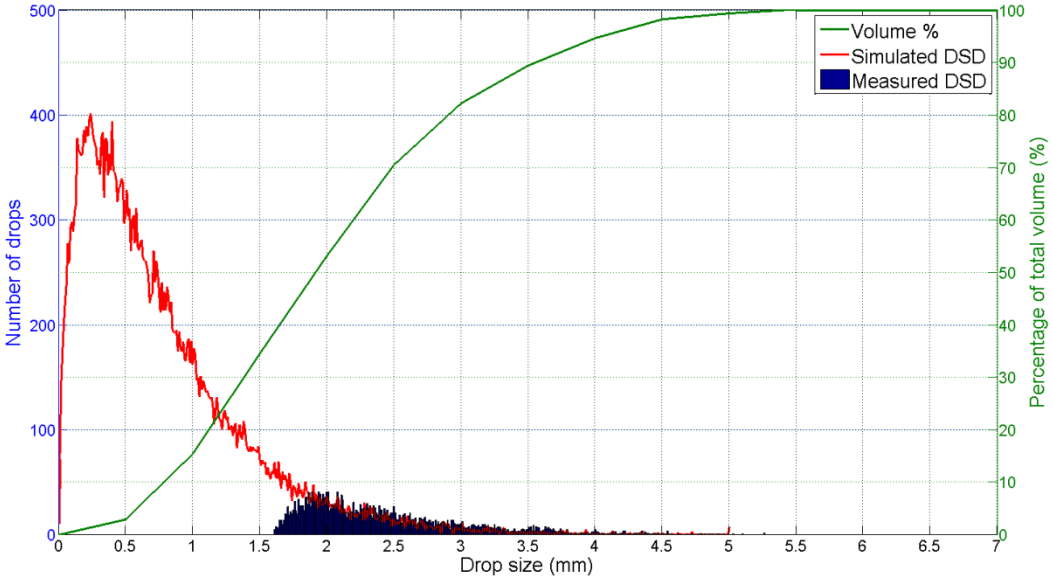

Figure 21: Measured DSD vs. Simulated DSD and the cumulative percentage of the total volume based on the simulated DSD

It is clear that the smallest drop measured is above 1.5 mm in diameter. According to the simulated drop size distribution all drops above 1.5mm are responsible for approximately 65% of the total volume of this rain event. This would suggest that the there is an underestimation of the total sum if the simulated and measured drop size distribution are compared. However in this case the total volume of the measured drops exceeds the total volume of the simulated drops. This can be explained by the fact that the simulated drop size distribution is based on the data of a tipping bucket. A tipping bucket is not accurate in case of high rain rates, since it tends to miss water during the tip. This underestimation by the tipping bucket causes that the probability density function are based on intensities that are lower than the real rain intensity, causing a larger scale parameter of the gamma distribution, which means that there would be relative more larger drops than in the simulated drop size distribution from this example.

The uncertainty in the simulated drop size distribution makes this validation method only useful as an indication of what should be measured. If the peak of the measured drop size distribution would lay at e.g. 4mm then it is clear that the measured drop size distribution and the simulated distribution differ significantly, making the measured result not acceptable. The fact that the measured drop size distribution is fits the tail of the simulated drop size distribution gives additional confidence to these results.

6. Case study

To test the low cost disdrometer in an urban environment two case studies were conducted. For each case study, one configuration of the low cost disdrometer was used. For the EWI case study the Rainscan configuration was used, where for the Singapore case study the standalone version of the disdrometer was used. The results of the measurements are given in chapter 7: Results.

Case study: EWI

The faculty of Electrical engineering, Mathematics and Computer Science (EWI) is situated on the campus of Delft University of Technology, the Netherlands ($51.99872° N, 4.37356° E.$). The high rise building of EWI is 90 meters in height and the highest building of Delft. The low rise building of EWI is situated on east side of the high rise and has a height of approximately 15 meters.
The dominant wind direction is West to South-West and perpendicular on EWI where the low rise building is positioned on the leeside of the high rise building.

Figure 22: Faculty of Electrical engineering, Mathematics and Computer Science

It is well known within the Delft community that the wind around the faculty of EWI can be very strong. It is expected that the wind has a strong influence on the spatial distribution of rainfall around the building. Observations strengthen this expectation, Figure 23 shows a clear pattern of rain on the red-side of the high rise building (difference between dark and light red). Also on top of the low rise building the effect of wind is clearly visible. Figure 24 and Figure 25 shows that there is settling of sand in the shadow of the high rise building, probably because the wind is weaker on the leeside which make it possible for the sand, carried by the wind, to settle.

Figure 23: Effect of rain and wind on side of EWI building

Figure 24: Roof of elevator shaft NOT in shadow of high rise

Figure 25: Roof of elevator shaft IN shadow of high rise

The expectation that wind plays a strong role in the distribution of rainfall around the building makes the faculty of EWI an interesting location to test the functionality of the low cost disdrometer.

25 disdrometers were placed on the roof of the low rise building, with half of the disdrometers placed in the shadow of the high rise building, see Figure 26. As a reference measurement, two tipping bucket rain gauges were installed on the same roof, of which one tipping bucket was placed in the shadow of the building and the other was placed at a distance of approximately 100 meters from the high rise building.

The roof of the low rise building has the benefit that it is not accessible for public, so the chance that disdrometers are stolen or that measurements are interfered by human activity is negligible.

The disdrometers placed on the roof are placed according to the RainScan configuration (see Chapter 3: Design)

Figure 26: Aerial view of test location, indicated by red box

Case study: Singapore

The standalone disdrometer was tested in Singapore ($1.29617° N, 103.77454° E.$) from the end of August till mid September to provide an idea of how the low cost disdrometer and the data logger perform in tropical rain events.

The standalone disdrometer was attached to a pile on the roof of an university building. Next to disdrometer a tipping bucket is located, see Figure 27.

Figure 27: Disdrometer located next to tipping bucket, Singapore

7. Results

In this chapter the results of the case studies are given. These results show that for all measurement there is a significant underestimation of the amount of rainfall observed with the disdrometer in comparison with the reference measurements, which indicate a problem in either the design of the sensor, the logger or in the calibration curve. Therefore the data is not used to investigated any spatial distribution of rain in the urban area. This chapter only shows an overview of the measurement, further elaboration on the data can be found in Chapter 8: Analyses.

Before the measurements of the disdrometer can be compared to the tipping bucket the output of the disdrometer has to be converted into individual drop diameters with the calibration curve found in chapter 4: Calibration. If the individual drop diameters are known, the total rain depth can easily be calculated (see Chapter 1: Introduction).

Case study: EWI

The measurements in the EWI case study are conducted in July and at the end of August 2010. Figure 28 gives an overview of the cumulative rain depth of all 25 disdrometer and the tipping bucket during the measurement period. From these figure it is clear that there is a significant underestimation of the amount of rainfall by the disdrometers. This indicates that there is a problem with the design of the sensor, logger or that the calibration curve is not correct. Therefore the data is not used for investigation of spatial patterns around the high rise building of EWI, but only used as input to define any possible problems, see Chapter 8: Analyses.

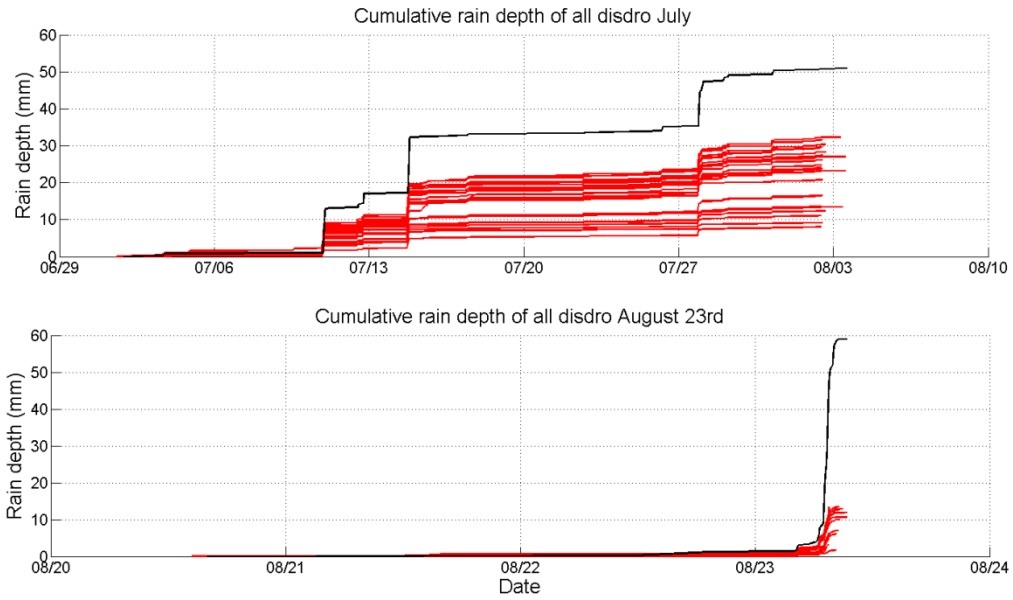

Figure 28: Cumulative rain depth of tipping bucket (black) and 25 disdrometers (red) for July (top) and end of August (bottom).

A closer look to the data measured with the disdrometer and tipping bucket closest to each other are given here. This is also the data on which the analyses in Chapter 8 are based.

Figure 29 shows the result of the measurements performed in July 2010. The top graph in the figure shows the moment individual drops of a certain drop size occurred, the bottom graph gives the cumulative rain depth of both the disdrometer and the tipping bucket. Over the given period the disdrometer observed approximately 37.000 drops with a total rain depth of about 28mm. The tipping bucket measured in the same period a total rain depth of 53mm.

Figure 30 shows the results of the measurements at the end of August 2010. The disdrometer observed approximately 13.000 drops with a total rain depth of 12mm. The tipping bucket measured in the same period a total rain depth of almost 60mm.

The moment that the drops were registered by the disdrometer seems to match with the moments that there is rainfall measured with the tipping bucket. However the amount of rainfall measured by the disdrometer is significantly less than the tipping bucket observed.

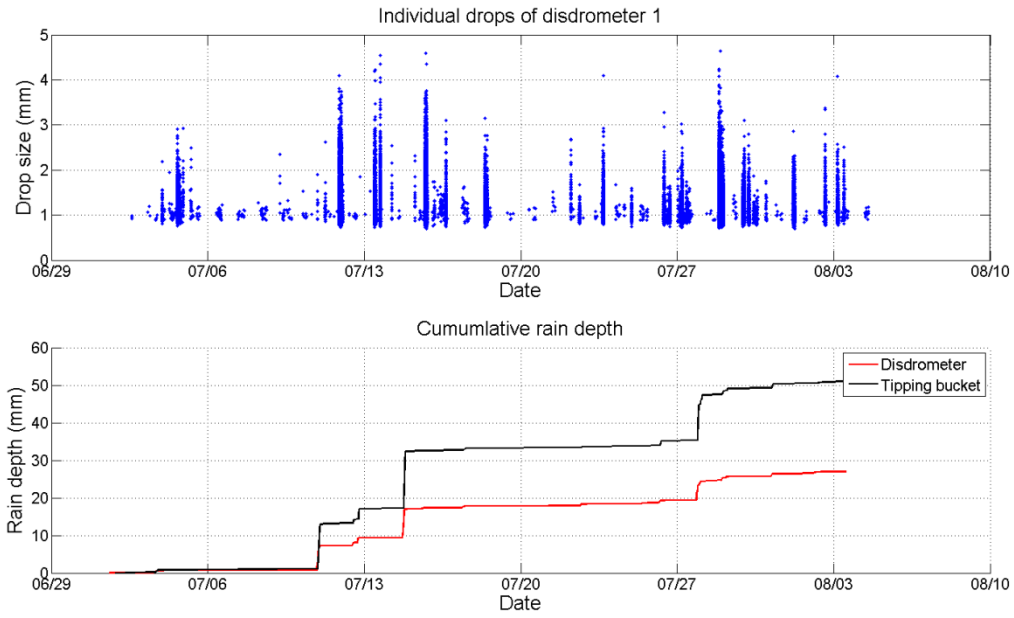

Figure 29: Individual drop recordings by disdrometer and cumulative rain depth of tipping bucket and disdrometer in the period of 01/07/2010-03/08/2010

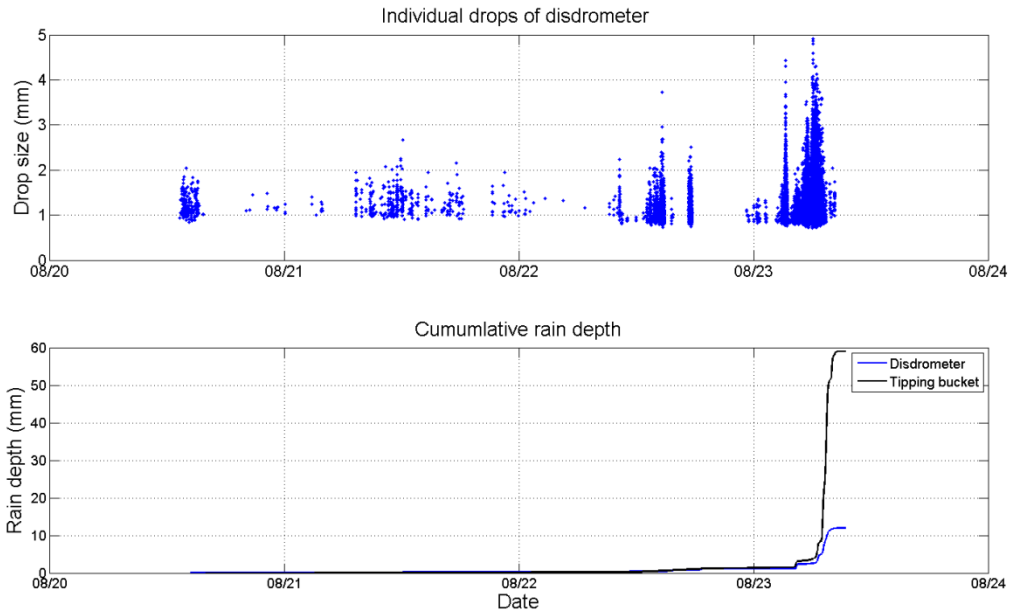

Figure 30: Individual drop recordings by disdrometer and cumulative rain depth of tipping bucket and disdrometer in the period of 20/08/2010-23/08/2010

Case study: Singapore

The measurements with the standalone version of the disdrometer in Singapore are conducted in the period August 26 – September 17. In this period the tipping bucket recorded a total rain depth of 220 mm. In this period the disdrometer recorded approximately 75.000 drops. The total rain depth observed with the disdrometer is 44mm. The cumulative rain depth of the tipping bucket and the disdrometer over the given period are shown in Figure 31.

According to the timestamps of the disdrometer, the disdrometer stopped working on September 16, the last timestamp given however consists of only zeros. According to the tipping bucket there was an extreme rain event on September 17 and was there no rain on September 16.

From the measurements with the standalone version of the disdrometer we can also conclude that there is a significant underestimation of the amount of rain fall with the disdrometer.

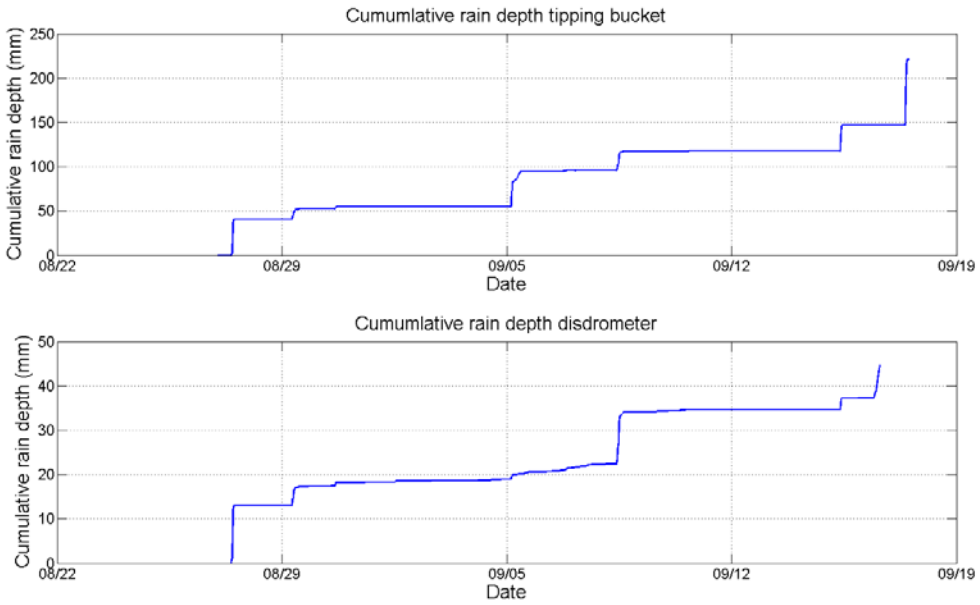

Figure 31: Cumulative rain depth of tipping bucket and disdrometer, Singapore 26/08/2010-17/09/2010

8. Analysis

From the results of both the EWI and the Singapore study case it is clear that the disdrometer measures significantly less than the tipping bucket over the same period. This problem could be caused by a problem in the design of the sensor or the logger, or a wrong interpretation of the data due to an incorrect calibration curve. To get more insight in the problem and to specify the cause, the data of the measurements are analyzed further with respect to rain intensity and the observed drop size distribution. Also some extra tests with the logger were performed.

Rain intensity

If we take a close look at the cumulative rain depth of the disdrometer which is closest to the tipping bucket, see Figure 29, it appears that the disdrometer stays behind on the tipping bucket only at the moments that the 'step' in the cumulative is more than approximately 3-5mm. Figure 32 shows that when the cumulative line of the disdrometer is cut in parts and shifted over the vertical it perfectly fits the cumulative rain depth of the tipping bucket. This suggests that the disdrometer only gives an underestimation of the amount of rain for relative high rain intensities. This is confirmed by Figure 33 and Figure 34, which show the rain intensity observed by the tipping bucket and the disdrometer. For relatively low intensities the observed intensity of the tipping bucket and the disdrometer are in the same order of magnitude. Where for intensities above 10mm/hr the disdrometer has problems to observe the same intensity as the tipping bucket.

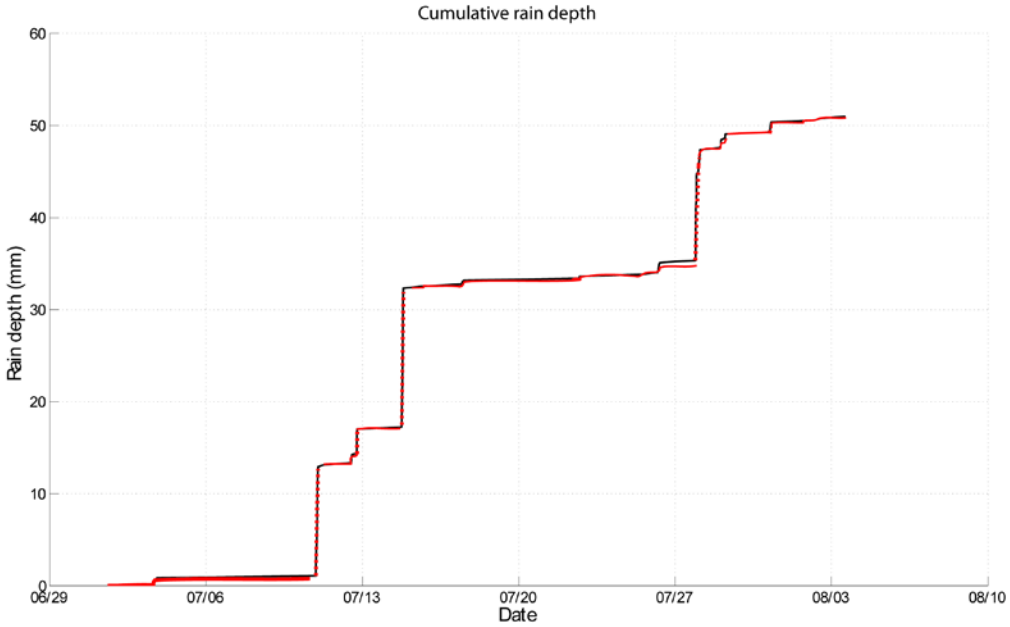

Figure 32: Cumulative rain depth of disdrometer cut in parts and shifted over the vertical (dashed line) red: disdrometer, black: tipping bucket

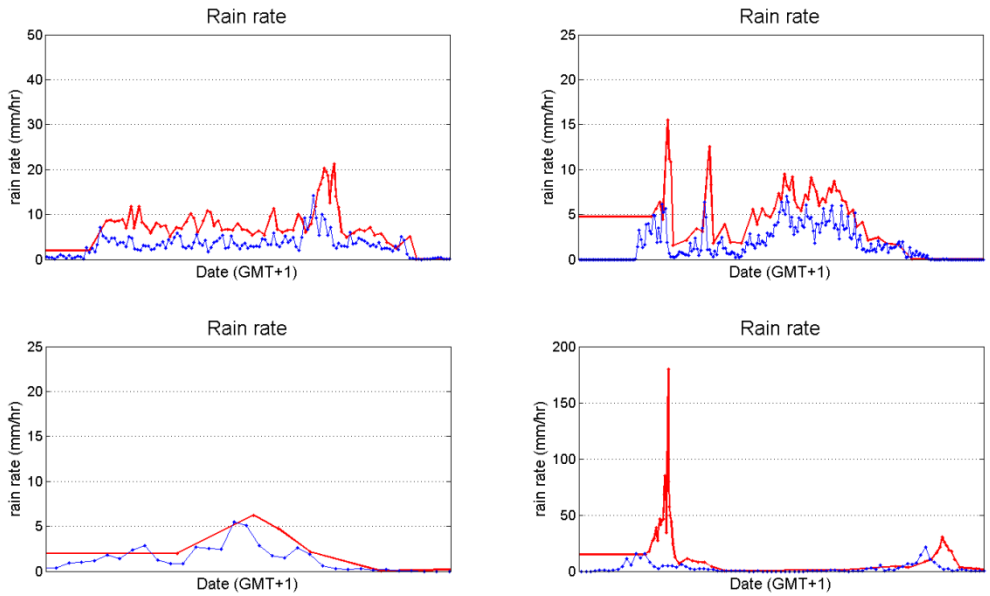

Figure 33: Rain intensity according to tipping bucket (red) and disdrometer (blue) for some rain events in July 2010

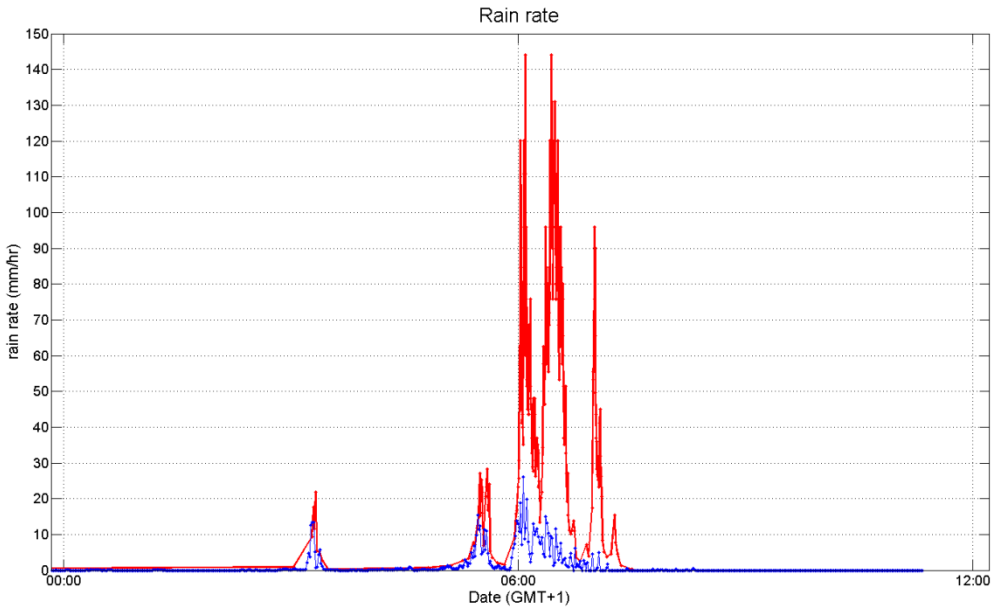

Figure 34: Rain intensity according to tipping bucket (red) and disdrometer (blue) for rain event on August 23rd 2010

The maximum observed rainfall intensity of the disdrometer is 26mm/hr, where the tipping bucket at the same moment observes an intensity of 170mm/hr, see Figure 34. However this seems not to be a fixed maximum, since the measured intensity by the disdrometer does not always reach 26mm/hr if the intensity measured by the tipping bucket is above 26mm/hr.

Drop size distribution

With the validation method described in chapter 5: Validation, it is possible to compare the drop size distribution measured by the disdrometer with a simulated drop size distribution based on the data of the tipping bucket.

Figure 35 shows the simulated drop size distribution and the measured drop size distribution by the disdrometer for a rain event with low intensity on September 27. The intensity of this rain event did not exceed 2mm/hr. The measured amount of drops by the disdrometer is 2300 and the minimum drop size is 0.9mm. The total amount of drops in the simulated DSD is approximately 55.000. However, the amount of drops in the simulation larger then 0.9mm is 2200, which is more or less equal to the amount measured by the disdrometer. The volume presented by the drops larger then 0.9mm is approximately 90% of the total volume of the simulated DSD.

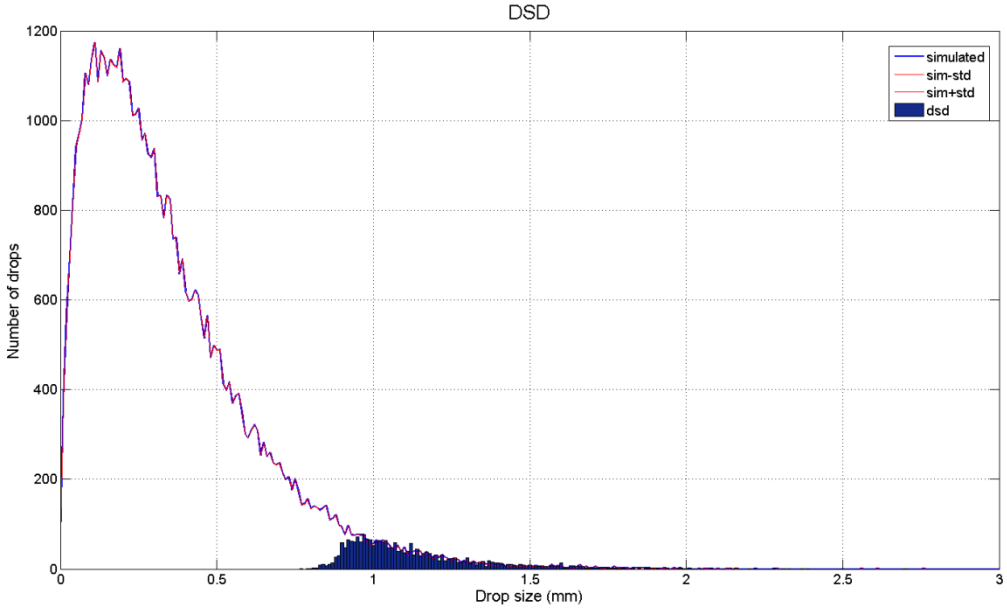

Figure 35: Simulated DSD vs. Measured DSD for a low intensity rain event on September 27th

Figure 36 shows the comparison between the measured and simulated drop size distribution of August 23rd. The total amount of drops in the simulated drop size distribution is approximately 140.000, where there are only 10.000 drops recorded by the disdrometer. The number of drops larger then 0.9mm for the simulated DSD is 36.000. So for the high intensity rain event a lot of drops are missing, which explains why the total rain depth measured by the disdrometer for this rain event is just a fraction of the rain depth measured by the tipping bucket, see Figure 30.

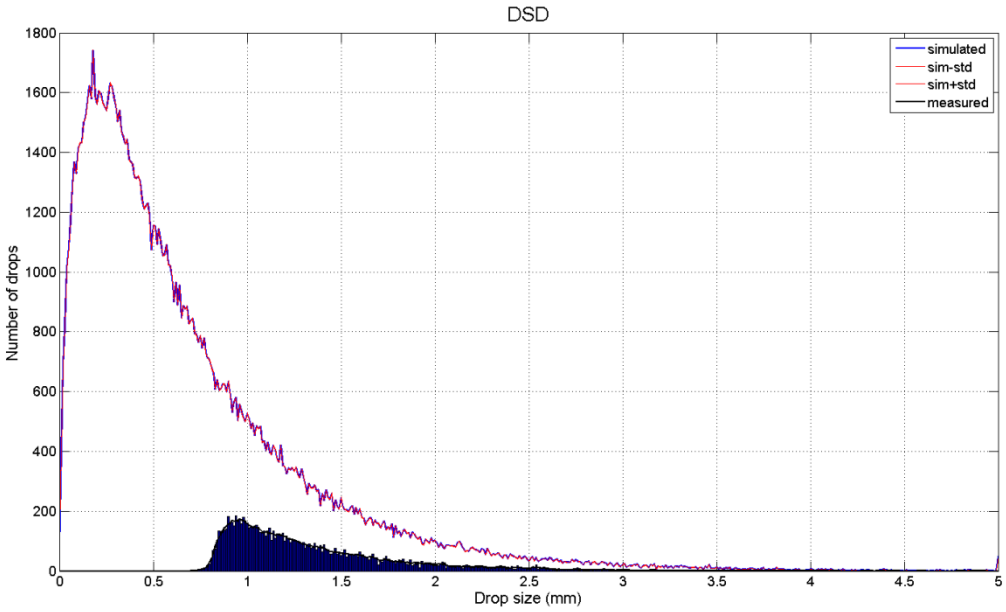

Figure 36: Simulated DSD vs. measured DSD for a high intensity rain event on August 23rd

The missing drops in the of 0.9mm-5mm add up to a total rain depth of 48mm, which is together with the 12mm recorded rain depth more or less equal to the observed rain depth of the tipping bucket, see Figure 30.

The fact that the measured DSD in Figure 35 fits the simulated DSD gives confidence that the conversion from output data of the disdrometer to drop diameter with the calibration curve is correct.

Sensor

In order to test if the sensor itself is the cause of the underestimation during high rain intensity the sensor has to be tested without the logger. Therefore a measurement is performed where the data is collected with an audio recorder. This way of data acquisition was also used by Degen for the first prototype.

The measurement conducted with the current prototype was during a rain event with a low intensity on September 30, 2010. The intensity did not exceed 2mm/hr during the event. For this event a total amount of 3mm was measured with the tipping bucket and a totaling rain gauge. From the soundfile, recorded by the audio recorder, approximately 9000 drops were extracted, summing up to a rain depth of also approximately 3mm.

Figure 37 shows the drop size distribution of the measurement done on September 30th with the current prototype and an audio recorder, also the corresponding simulated drop size distribution is shown in this figure. As a comparison the results from the first prototype of July 7th 2009 are also given in Figure 37.

From Figure 37 we can conclude that both the first prototype and the current prototype give a good result, since both DSD fit, a part of, the simulated DSD. The smallest drop observed by the current prototype with an audio recorder as data acquisition is 0.6mm, which is smaller than the minimum drop size when the logger is used to collect data. This could be caused by the height of the threshold set in the software of the logger.
The smallest drop observed by the first prototype is 1.6mm from which we can conclude that the

current prototype is more sensitive than the first prototype and therefore able to measure the drops that represent approximately 95% of the total amount of rain.

Because the measured data fits the simulation DSD it can be stated that the observed *radius effect* and *puddle effect*, described in chapter 3: Design, does not has a noticeable influence on the measured data.

Although the measurement with the current prototype and the audio recorder is only conducted for a rain event with a low intensity, there is no reason to believe that the underestimation during high intensity is caused by a problem in the design of the sensor.

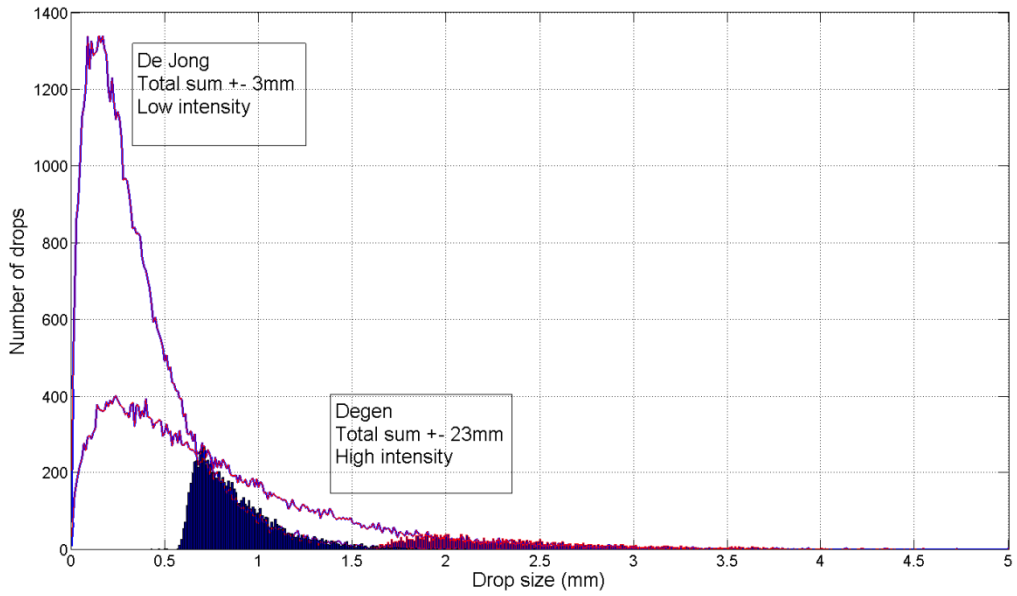

Figure 37: Comparison between first and current prototype, data acquisition with audio recorder

Logger

To test the logger separate from the sensor audio files can be used as a signal input. Instead of connecting the logger with the sensor, the logger is connected to the e.g. the computer with a mono audio plug.

To illustrate the difference between what the audio recorder and the data logger measures, the audiofile is used as an input for the data logger. Figure 38 shows how the audiofile recorded on September 30th is interpreted by the data logger. This confirms that the threshold set in the software of the logger is set to high.

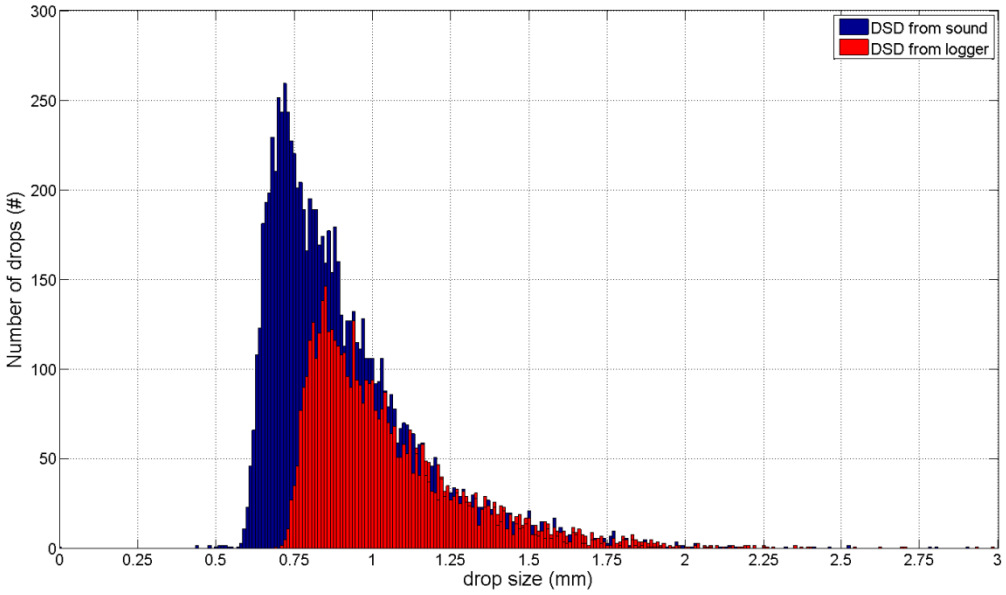

Figure 38: Sound used as input logger

To measure the maximum capacity of the logger a constant noise that was loud enough to trigger the logger, with a length of 60s was used as input. The maximum length of a drop signal was 12ms, when the logger is processing the signal and transferring the data it is not able to start recording a new drop. If the logger is ready with processing one drop signal it immediately starts with the next recording. In the 60s of loud noise, 1850 'drops' were recorded. For every drop signal the logger needed a total of 32ms, so the processing time of each signal is 20ms. So for each second a maximum of 30 drops could be processed if the drops are sequent.

The highest amount of drops measured by the disdrometer is 260 for one minute, on August 23rd. At the same moment the tipping bucket recorded a rain intensity of 150mm/hr. The expected number of drops that have to be measured at such intensity is 1500, which implies that the disdrometer missed 1250 drops during this specific minute. This would mean that there would be on average 5 drop impacts during each calculation time of a recorded drop. Since the calculation time of the recorded drops only takes about 15% of the time in this minute, this seems to be impossible. It's more likely that the logger is only overloaded for a short amount of time, but that it is not able to recover from this stage. The fact that the disdrometer does not reacts on the peak intensities after the first peak, see Figure 34, strengthens this thought.

However it is obvious that the data logger did not performed as it should, it is not clear what exactly is wrong with it.. During the calibration process in the lab it was not observed that the data logger was missing a significant number of drops. From the results of the logger and the comparison with the data from the audio recorder it can be concluded that the problem in the logger was not caused by the threshold set in the software, since the data logger was missing drops over the whole range and not only the small drops what should be the case if the threshold was set to high. The height of the threshold of the logger could be reduced to be able to record smaller drops.

9. Conclusion

The main conclusion drawn from the conducted research is that the sensor of the current prototype performs better than the first prototype and that in general the principle works. However the logger designed for the disdrometer is not capable of giving a right representation of the actual rainfall under all circumstances. Before the low cost disdrometer can operate in the field for longer periods, first the problems with the data logger have to be solved.

The design of the disdrometer has been improved in terms of sensitivity and the method of production. From the measurements with the audio recorder it is observed that the smallest drop measured by the current prototype is 0.6 mm, where the smallest drop measured by the first prototype was 1.5mm. The radius effect and puddle effect are points of interest, however these effects do not have a visible effect on the measurements.

Calibration of the disdrometer showed a clear relation between the signal energy of a drop and the size of the drop. The uncertainty in the calibration curve can be decreased by calibrating the disdrometer with the help of an optical disdrometer.

The validation method gives an indication of what the drop size distribution of a rain event should look like if there is no disdrometer available. The method is based on the data of a tipping bucket. With this method it is possible to simulate an expected drop size distribution which can be used to validate the measurements of the disdrometer.

The results from the measurements in the case studies showed a large underestimation of the total amount of rain. This underestimation only takes place during rain events with high rain intensity. The maximum intensity measured with the disdrometer is 26mm/hr. During the measurements the maximum capacity of the logger was never reached, which is probably caused by a hardware and/or software problem in the logger.

Future work that has to be done will be described in Chapter 10: Future work.

10. Future work

The first results of the disdrometers show that there is potential. However, there are still a lot of aspects that have to be investigated further. At the time of writing most of this work is already in process.

- Most important work that has to be done is the debugging of the logger, to make it possible to perform tests for all rain intensities.
- When the logger is debugged, more data have to be acquired to investigate the variability between sensors and to get more insight in the accuracy.
- The disdrometer has to be tested to define the sensitivity for temperature, air pressure, radiation, wind etc.
- Define the durability of the disdrometer.
- The design has to be optimized to reduce the radius and puddle effect and to make the disdrometer suitable for an automated production process.
- The calibration of the disdrometer can probably be done with an optical disdrometer, to reduce the source of errors in the calibration process. An optical disdrometer gives information about the size and speed of individual drops and has a very high accuracy.

There is more work to be done before the low cost disdrometer is a final product, but in this stage of development most of this work is not relevant yet, but an idea of the amount of work that has to be performed can be concluded from the vision of the low cost disdrometer as a final product.

Vision
As a final product the low cost disdrometer should be a *plug and play* tool, which can operate in a complete network of low cost disdrometers and other sensors. To make this possible there should be a main unit that acts as a backbone where different sensors can be connected to. This backbone needs to have its own (renewable) power supply to last a long time without maintenance. The data from each main unit has to be transmitted to a central server from where the data is processed and published. The main unit should be provided with a location tracker, such as GPS, so that it is known where the data is coming from. If the data is received by the server en processed it can be published for example on the internet as maps with contour lines of rain depth and rain intensity or in more detail as a drop size distribution per station for a specific time. The data could in the same way be combined with data from other stations such as those from the Meteorological service, or even with pictures people made during rain events or flooding to get even more connected to the data.

References

Beard, K. V. (1976). "Terminal velocity and shape of cloud and precipitation drops aloft." Journal of the Atmospheric Sciences **33**(5): 851-864.

Beard, K. V. and C. Chuang (1987). "A New Model for the Equilibrium Shape of Raindrops." Journal of the Atmospheric Sciences **44**(11): 1509-1524.

Bornstein, R. and Q. Lin (2000). "Urban heat islands and summertime convective thunderstorms in Atlanta: Three case studies." Atmospheric Environment **34**(3): 507-516.

Brandt, C. J. (1990). "Simulation of the size distribution and erosivity of raindrops and throughfall drops." Earth Surface Processes & Landforms **15**(8): 687-698.

Degen, C. (2009). Development of a low-cost acoustic rain gauge. Internship report, Delft University of Technology.

Gautschi, G. (2002). Piezoelctric Sensorics: Force, Strain, Pressure, Acceleration and Acoustic Emission Sensors, Materials and Amplifiers, Springer.

Gunn, R. and G. D. Kinzer (1949). "The Terminal Velocity of Fall for Water Droplets in Stagnant Air." Journal of Atmospheric Sciences **6**: 243-248.

Henson, W., G. Austin, et al. (2004). "Development of an inexpensive raindrop size spectrometer." Journal of Atmospheric and Oceanic Technology **21**(11): 1710-1717.

Joss, J. and A. Waldvogel (1967). "Ein Spektrograph für Niederschlagstropfen mit automatischer Auswertung." Pure and Applied Geophysics PAGEOPH **68**(1): 240-246.

Kourtellis, A. G., T. Kasparis, et al. (2005). Disdrometer calibration using an adaptive signal processing algorithm.

Lavergnat, J. and P. Golé (1998). "A Stochastic Raindrop Time Distribution Model." Journal of Applied Meteorology **37**(8): 805-818.

Licznar, P., J. Łomotowski, et al. (2008). "Microprocessor field impactometer calibration: Do we measure drop's momentum or their kinetic energy?" Journal of Atmospheric and Oceanic Technology **25**(5): 742-753.

Marshall, J. S. and W. M. Palmer (1948). "The distribution of raindrops with size. ." Jounal of Meteorology **5**: 165-166.

Mason, B. J. (1978). "Physics of a raindrop." Physics Education **13**(7): 414-419.

Niemczynowicz, J. (1999). "Urban hydrology and water management - present and future challenges." Urban Water **1**(1): 1-14.

Oppenheim, A. V. and A. S. Willsky, Eds. (1997). Signals&Systems. Signal Processing Series, Pretenice-Hall, INC.

Salmi, A. and J. Ikonen (2005). New piezoelectric Vaisaila RAINCAP precipitation sensor. 19th Conference of hydrology, San Diego.

Schilling, W. (1991). "Rainfall data for urban hydrology: what do we need?" Atmospheric Research **27**(1-3): 5-21.

Uijlenhoet, R. and J. N. M. Stricker (1999). "A consistent rainfall parameterization based on the exponential raindrop size distribution." Journal of Hydrology **218**(3-4): 101-127.

WMO (2008). WMO guide to meteorological instruments and methods of observation.

List of figures

Websites

http://www.tahmo.org/ – Information about the Tahmo project

http://www.cognisys-inc.com – Information about the StopShot module

http://chdk.wikia.com – Information about how to hack a Canon Powershot camera

Appendix 1: Prototypes

First prototype: (made by Coen Degen)

The piëzo electric disk used here has a diameter of 35mm. The disdrometer is completely made from crystal-clear cast resin. The crystal clear cast resin is formed in silicon molds.
The production of this prototype is time intensive and the use of resin makes it hard to make two identical disdrometers.

Second prototype:

The lower part of the disdrometer is replaced by a piece of PVC pipe. The pipe is filled with resin. The hat of the prototype is still made of crystal clear cast resin. The prototype is already easier to produce than the first prototype.
This prototype had a very high triggering level. Most impacts did not exceed the noise level.

Third prototype:

This prototype is in principle the same as the second prototype, it only has less mass. There is no resin in the pipe and the hat is thinner. Because the hat of the sensor is a lot thinner than the previous prototype, the sensor is able to measure smaller drops.
The use of crystal clear cast resin still makes it hard to make two identical disdrometers.

Fourth prototype:

The crystal clear cast resin hat is replaced by a PVC version. There is no resin used anymore. The sensor is extended with a case for the logger. The sensor also seems to register drop impacts on the logger casing.

Fifth prototype:

Same as the fourth prototype, but with a longer PVC pipe between the sensor hat and the logger casing. Still there is the problem that drops hitting the logger casing are registered.

Sixth prototype:

Same as the fifth prototype, but with a piece of silicon between the PVC pipe and the sensor hat. There are still drops registered that hit the logger casing.
The used silicon seems to have a negative effect on the piëzo electric disk, it corrodes in a short amount of time.

Current prototype:

No silicon and crystal clear cast resin used. The logger casing is separate from the sensor. The casing of the piëzo electric disk is completely made of PVC. The sensor is easy to build and it is possible to make two identical disdrometers.